

Deviations from Debye's specific heat due to excess energy fluctuations

Ralph V. Chamberlin¹ and Sumiyoshi Abe^{2,3,4}

¹Department of Physics, Arizona State University, Tempe, AZ 85287-1504, USA

²Department of Physics, College of Information Science and Engineering, Huaquiao University, Xiamen 361021, China

³Institute of Physics, Kazan Federal University, Kazan 420008, Russia

⁴Department of Natural and Mathematical Sciences, Turin Polytechnic University in Tashkent, Tashkent 100095, Uzbekistan

Abstract: Measured specific heats often exceed Debye's T^3 -law, even in high-purity single crystals. Analogous excess energy fluctuations in molecular dynamics (MD) simulations of crystals with no defects come from fast energy modulations involving next-nearest-neighbor atoms. Here, a theory is developed for these modulations, based on time- and phase-averaging followed by thermal averaging. This order of averaging is guided by evidence from the simulations and various experimental techniques showing that localized excitations are decoupled from the heat bath. Emergent nonextensivity is interpreted by analogy with anomalous diffusion. The theory modifies the standard relation between energy fluctuations and specific heat, giving good agreement with the simulations and new insight into many measurements. The theory may also provide a basis for understanding excess specific heat in amorphous materials and anomalous noise in quantum devices.

The standard theory for describing specific heat, C , of crystals at cryogenic temperatures ($T \ll 300$ K) is Debye's treatment of quantized harmonic modes (phonons) [1,2]. Debye's theory gives $C \propto T^3$ as $T \rightarrow 0$. The accuracy of this theory should increase with decreasing T , but many measurements, even on ultra-pure single-crystal dielectrics, show excess C at $T \ll 1$ K [3-5]. The authors of Ref. [3] attribute this excess to their technique of measuring time-resolved specific heat as being "...a very sensitive test for residual impurities in perfect crystals." However, molecular dynamics (MD) simulations of crystals with *no impurities* show an analogous excess in energy fluctuations [6]. Here we develop a theory that quantitatively explains the excess energy fluctuations in the simulations and gives insight into measured behavior.

Canonical-ensemble theory contains a formal identity connecting specific heat and energy fluctuations [7], which we call the $C \leftrightarrow (\Delta E)^2$ relation. The theory we propose adds a correction to this relation. The correction comes from anharmonic interactions between next-nearest neighbor (nnn) atoms that adiabatically modulate the harmonic interactions between nearest-neighbor (nn) atoms. The resulting behavior involves time- and phase-averaging over the fast anharmonic modulations, then thermal averaging over the slower harmonic modes. The key point is that the modulated energies are fast enough to be effectively decoupled from the heat bath, consistent with evidence from simulations [6] and many measurements [3-5,8-10]. In other words, the energy modulations are uniformly distributed degrees of freedom, without Boltzmann's factor. For simplicity, the modulations are treated semiclassically, even in the quantum regime.

The well-known excess specific heat in glasses [1,11] is often attributed to defects that yield tunneling two-level systems (TTLS) [12-16]. Similarly, excess noise in quantum devices, such as qubits and single-particle detectors [17-21], has also been attributed to TTLS. However, the source of TTLS in most materials remains unknown, especially in pure crystals, with behavior that may be refuted by experiment [14,15,22]. Here, we show that analogous excess energy fluctuations in MD simulations of crystals *without defects* are quantitatively explained by anharmonic interactions from nnn atoms that modulate harmonic modes, indicating an intrinsic mechanism. Moreover, our model explains the observation that excess specific heat is much more prominent in amorphous materials, where essentially all interactions are anharmonic so that the motion of every atom strongly modulates the energies of most neighbors.

The main experiment that guides our theory involves time-resolved specific heat [3-5]. These measurements establish the importance of multiple effective temperatures inside a single sample. In high-purity single crystals at $T \ll 1$ K, the short-time (initial) specific heat agrees with Debye's theory, but the long-time (equilibrium) specific heat deviates from

Debye's theory. Additional insight into our theory comes from experiments showing that the excess specific heat involves localized normal modes [23- 28]. Further evidence comes from neutron scattering measurements that show a sharp reduction in the correlations between nnn atoms compared to nn atoms [29], as needed for the relatively independent motion of nnn atoms in our theory.

In FIG. 1, we present results from measurements [3-5] of specific heat on five high-purity single crystals. The inset shows a sketch of the “box” model for interpreting the behavior [10]. An electrical pulse gives a fixed amount of Joule heating to the resistor on one side of the sample, with temperature change (δT) measured as a function of time on the other side. Each box in the sketch represents a set of localized degrees of freedom that have local temperatures (T_i) and heat resistor (time constant, τ_i) that couples it weakly to the heat bath. The measurements are on a quartz crystal at a base temperature of $T \sim 0.2$ K. Note how the change in temperature, δT , starts at zero, rises sharply until it reaches a peak at $t \sim 0.01$ ms, then recovers towards zero in multiple stages. The overshoot and peak at ~ 0.01 ms are due to the initial arrival of ballistic phonons from the heater. After the peak, the added heat becomes evenly dispersed among all phonons that form the heat bath, allowing δT to stabilize at an initial plateau (solid black line) that equals δT_D from Debye's theory. However, starting at $t \sim 1$ ms, δT relaxes again, subsequently reaching an equilibrium plateau (dashed red line) at $t > 10$ ms, which gives the total specific heat of the sample. Finally, at much longer times ($t \gg 100$ ms, not shown), δT returns to zero as the excess heat flows out of the sample through the wires that connect it to the cryostat.

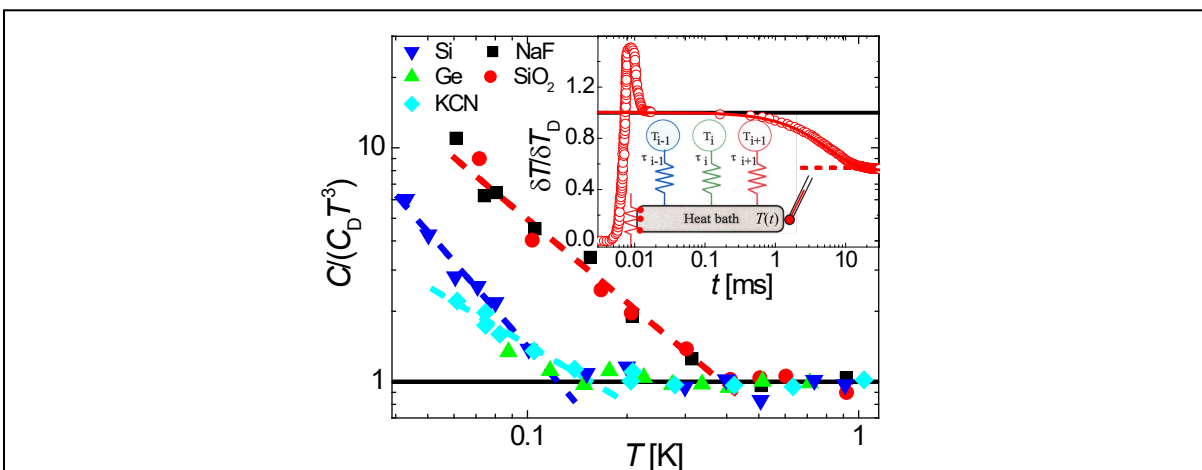
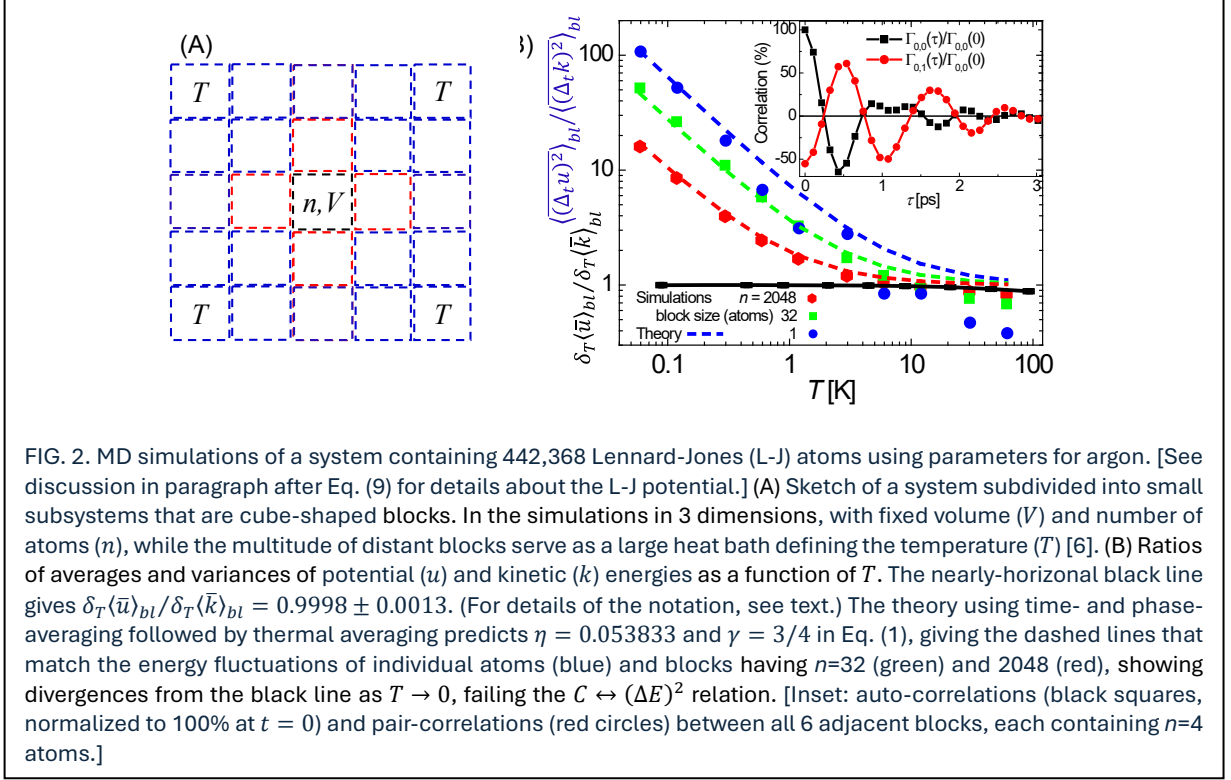


FIG. 1. Measurements of specific heat from five high-purity single crystals, given in the legend [3-5]. [Inset: sketch depicts a model for interpreting the behavior [10]. Plot shows δT normalized by Debye's T^3 -law, δT_D (solid black line), as a function of time from measurements of an SiO_2 crystal at ~ 0.2 K. Red lines show long-time-limit behavior (dashed) and an exponential fit to the data (solid).] Filled symbols (given in the legend) show the equilibrium specific heat as a function of temperature, normalized by Debye's specific heat [solid line at $C/(C_D T^3) = 1$]. Dashed lines show power-law fits to the excess specific heats (with colors identified in the legend), showing divergence from Debye's theory as $1/T \rightarrow \infty$: $C/(C_D T^3) - 1 = \alpha/T^\mu$. The exponents range from $\mu = 0.94 \pm 0.15$ for KCN to 1.64 ± 0.12 for Si, with an average of $\mu = 1.4 \pm 0.3$.

Because the specific heat is inversely related to δT [5], the inset of FIG. 1 shows that the equilibrium specific heat is significantly higher than its initial value. The initial value of C comes from the homogeneous heat bath of phonons that yield Debye's theory, while the equilibrium value has additional degrees of freedom. In fact, during the nearly-exponential relaxation connecting these plateaus (red curve during $0.1 \lesssim t \lesssim 10$ ms), the excess heat supplied to the sample is not flowing across the sample (heat bath equilibration occurs at $t \approx 0.01$ ms), and it is not flowing out of the sample (coupling to the cryostat occurs at $t \gg 100$ ms). Thus, the excess heat must be flowing from the heat bath into other degrees of freedom inside the sample. Net heat flows only if there is a temperature difference. Hence, this experiment establishes that there are multiple temperatures inside a sample that do not equilibrate to a common T until $t > 10$ ms. Therefore, while these localized degrees of freedom are relaxing, their thermal exchange with the heat bath is too slow to be governed by a single T . In other words, fast fluctuations of these localized degrees of freedom are *decoupled from the heat bath* due to their relatively weak thermal link, represented by heat resistors in the sketch in FIG. 1. The main part of FIG. 1 shows the temperature dependence of the equilibrium values of normalized specific heat from time-resolved measurements [3-5], which clearly deviate from Debye's T^3 -law at low T .

Figure 2 (A) is a sketch showing how a large simulation can be subdivided into smaller subsystems (blocks) to study local thermal behavior. Specifically, the fixed volume and number of particles in each block should yield canonical-ensemble behavior, with the multitude of distant blocks providing the large heat bath needed to define T . However, MD simulations of several models [6] show significant deviations from the predictions of the canonical ensemble, especially at low T .

The main part of FIG. 2 (B) shows results from MD simulations of the Lennard-Jones (L-J) model as a function of temperature for three different block sizes, given in the legend, with parameters chosen for argon [30]. The equipartition theorem predicts that each quadratic degree of freedom should have a T -dependent component of $k_B T/2$. The notation we use is as follows. k and u are kinetic and potential energies, respectively. The overbar, angled brackets, and δ_T denote, respectively, time average, arithmetic mean over all blocks (subscript bl), and temperature difference $\delta_T Q \equiv [Q(T + \delta T) - Q(T)]$ ($Q = u, k$), with $\overline{(\Delta_t Q)^2} \equiv \overline{(Q(t) - \bar{Q})^2}$. At $T < 10$ K, the black line (with error bars) near unity gives $\delta_T \langle \bar{u} \rangle_{bl} / \delta_T \langle \bar{k} \rangle_{bl} = 0.9998 \pm 0.0013$. This ratio of partial specific heats from u and k is in excellent agreement with the equipartition theorem. In fact, each average energy separately agrees with the equipartition theorem. However, FIG. 2 (B) shows that the ratio of their fluctuations, $\overline{(\Delta_t u)^2}_{bl} / \overline{(\Delta_t k)^2}_{bl}$, diverges as $T \rightarrow 0$ reaching 10-100 times larger than



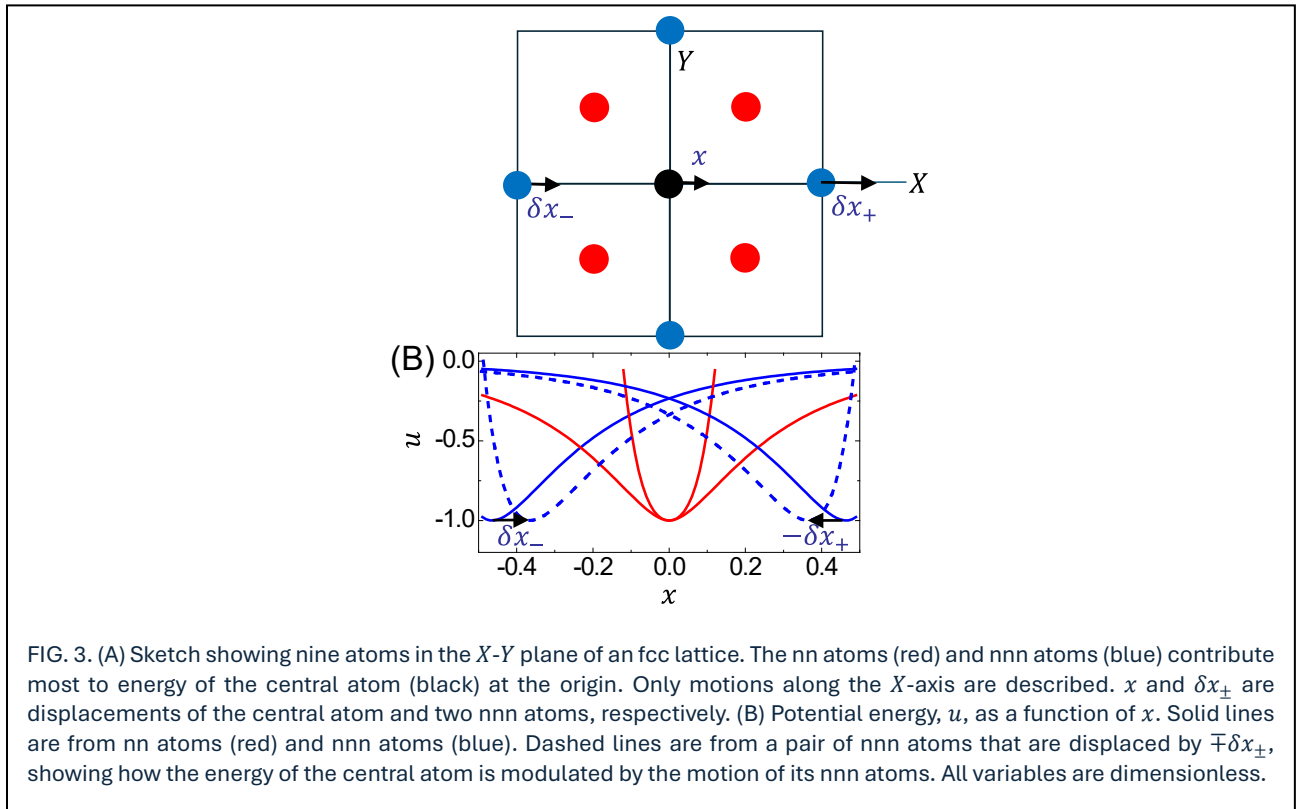
unity predicted by the $C \leftrightarrow (\Delta E)^2$ relation from canonical-ensemble theory. For blocks of n atoms, these excess fluctuations are empirically characterized by [6]

$$\frac{\langle(\Delta_t u)^2\rangle_{bl}}{\langle(\Delta_t k)^2\rangle_{bl}} - 1 = \eta n^{\gamma-1} \epsilon / k_B T, \quad (1)$$

with $\gamma = 0.75 \pm 0.05$ and $\eta = 0.054 \pm 0.004$.

The inset of FIG. 2 (B) clarifies the primary cause of excess fluctuations. We denote the auto-correlation function, and pair-correlation function between the central block and its six adjacent blocks, respectively, by $\langle \overline{u_0(t)u_0(t+\tau)} \rangle_{bl} \equiv \Gamma_{0,0}(\tau)$ and $\langle \overline{u_0(t)u_1(t+\tau)} \rangle_{bl} \equiv \Gamma_{0,1}(\tau)$. The ratio, $\Gamma_{0,0}(\tau)/\Gamma_{0,0}(0)$, starts at 100% and exhibits roughly damped harmonic relaxation with a period of ≈ 1 ps. While $\Gamma_{0,1}(\tau)/\Gamma_{0,0}(0)$ starts at $\lesssim -50\%$ and is primarily anticorrelated with $\Gamma_{0,0}(\tau)/\Gamma_{0,0}(0)$. Thus, more than 50% of the excess energy in the central block during its initial fluctuation comes from only six adjacent blocks. Therefore, it can be assumed that essentially 100% of the excess energy in the initial fluctuation comes from the surrounding “shell” of $3^3 - 1 = 26$ blocks that touch the central block, not from the large number of distant blocks needed for a well-defined T . In fact, during the first oscillation at $t \approx 0.5$ ps, the auto- and pair-correlations are equal in magnitude but opposite in sign, showing that most of the excess energy in the initial oscillation remains in the six neighboring blocks. Indeed, these strong anticorrelations establish the key result that excess energy fluctuations conserve local energy, effectively decoupled from the heat bath.

For many MD simulations [6], including those in FIG. 2, the excess energy fluctuations have three key features that infer their underlying mechanism. First, as shown in the inset of FIG. 2 (B), essentially all the energy in the excess fluctuation comes from the local shell of neighboring blocks, not from the large heat bath needed to define T . Thus, these excess fluctuations involve motions that are essentially decoupled from the heat bath. Therefore, the fluctuations are controlled by conservation of local energy, not by a well-defined T . Second, the excess fluctuations require interactions beyond nn atoms, arising abruptly (but smoothly) when the interaction starts to include nnn atoms. Third, the fluctuations in energy are positively correlated with particle density within each block inside the sample. This correlation, which also arises abruptly when the interaction starts to include nnn atoms, implies that excess energy fluctuations come from radially symmetric motion, i.e. a type of “breathing” mode for the atomic motions, as shown by the displacements $\mp\delta x_{\pm}$ in FIG. 3 (B). Note that the dominant influence of this breathing mode causes nnn motion to modulate the energy of the central atom, as represented by the solid and dashed blue lines in FIG. 3 (B).



Modulation of the harmonic motion of the central atom comes primarily from the relative motion its nnn atoms. This relative motion can be separated into in-phase and out-of-phase components. These two components have well-separated frequencies, as found in the simulations. Specifically, from figure 5 in Ref. [6], the frequency of the in-phase

component has a maximum of ≈ 0.5 THz, and goes to zero with increasing block size, while the largest out-of-phase component is nearly constant at $\omega/2\pi \approx 1.5$ THz. We identify the in-phase modes with the primary heat bath while the out-of-phase modes are effectively decoupled from this bath, consistent with the anticorrelated energies from simulations, e.g. inset of FIG. 2 (B), and from localized modes in many measurements [9, 10, 23-29].

Now, we develop a theory for the excess fluctuations in MD simulations. Consider a time-dependent potential energy for the motion in the x -direction of the atom at the origin in FIG. 3. Similar contributions in the other directions are equivalent. The potential energy has a harmonic term from nn atoms, $u(x) = ax^2$, plus a time-dependent modulation, $c(t)$, from nnn atoms. Neglecting any irrelevant constant offset, the modulated potential energy is

$$u(x, t) = ax^2 + c(t). \quad (3)$$

A linear dependence on distance (bx) does not appear explicitly in Eq. (3) due to the balance between the forces from opposing nnn atoms. Perfect balance requires that all nnn atoms maintain zero net displacement, $\delta x_+ = \delta x_-$. However, because nnn atoms tend to fluctuate independently, the same linear factor (b) arises in the time-dependent modulation, $c(t) = b \cdot (\delta x_+ - \delta x_-)$. The simulations show that the out-of-phase motion of nnn atoms is dominated by a single high-frequency, ω . Thus, the net displacement for the two nnn atoms on the x -axis in FIG. 3 (A) can be approximated by $\delta x_+ = A_+ \sin(\omega t + \alpha)$ and $\delta x_- = A_- \sin \omega t$. The amplitudes, A_{\pm} , come from the interactions between all nn atoms, which yield the harmonic modes forming the heat bath. These amplitudes can be replaced by their thermal averages, $\sqrt{\langle (A_{\pm})^2 \rangle_{th}} \equiv \mathcal{A}$, in each direction. The equipartition theorem gives

$$\mathcal{A} = \sqrt{k_B T / (2a)}, \quad (4)$$

so that the net modulation is

$$c(t) = b\mathcal{A}[\sin(\omega t + \alpha) - \sin \omega t]. \quad (5)$$

In contrast to the harmonic motions that are strongly correlated for nn atoms, especially for low-frequency motions, the higher-frequency breathing modes from nnn atoms are less correlated [29]. In addition, the initial phase, α , can be treated in the random-phase approximation, combined with time averaging to obtain the equilibrium properties of the crystal. The average potential energy of the central atom in FIG. 3 (A) now involves time- and phase-averaging (denoted by an overbar), followed by thermal averaging (denoted by angled brackets with subscript th). In the canonical ensemble, every contribution to energy is weighted by Boltzmann's factor. However, the modulations oscillate so fast that they are decoupled from the heat bath. After subsequent thermal averaging the mean potential energy becomes

$$\begin{aligned}
\langle \bar{u} \rangle_{th} &= \int_{-\infty}^{\infty} dx \frac{1}{Z} e^{-ax^2/k_B T} \int_0^{2\pi} \frac{d\alpha}{2\pi} \int_0^{2\pi/\omega} \frac{dt}{2\pi/\omega} \{ax^2 + b\mathcal{A}[\sin(\omega t + \alpha) - \sin \omega t]\} \\
&= \frac{1}{2} k_B T,
\end{aligned} \tag{6}$$

where $Z = \int_{-\infty}^{\infty} dx e^{-ax^2/k_B T}$. Because $\overline{c(t)} = 0$, Eq. (6) yields the familiar equipartition theorem, $\delta_T \langle \bar{u} \rangle_{th} / \delta T = k_B / 2$. However, $\overline{c^2(t)}$ is not zero, so that the second moment of u has an extra contribution:

$$\begin{aligned}
\langle \bar{u}^2 \rangle_{th} &= \int_{-\infty}^{\infty} dx \frac{1}{Z} e^{-ax^2/k_B T} \int_0^{2\pi} \frac{d\alpha}{2\pi} \int_0^{2\pi/\omega} \frac{dt}{2\pi/\omega} [ax^2 + c(t)]^2 \\
&= \frac{3}{4} (k_B T)^2 + b^2 \mathcal{A}^2.
\end{aligned} \tag{7}$$

Then, using Eq. (4) for \mathcal{A} , the variance of potential energy becomes

$$\begin{aligned}
(\bar{\Delta}u)^2 &\equiv \overline{(\overline{u} - \langle \bar{u} \rangle)^2}_{th} = \langle \bar{u}^2 \rangle_{th} - \langle \bar{u} \rangle_{th}^2 \\
&= \frac{1}{2} (k_B T)^2 + \frac{1}{2} \frac{b^2}{a} k_B T,
\end{aligned} \tag{8}$$

which results in the modified expression for potential energy fluctuations:

$$\frac{(\bar{\Delta}u)^2}{(k_B T)^2} = \frac{1}{2} + \frac{1}{2} \frac{b^2}{a k_B T}. \tag{9}$$

Thus, excess fluctuations diverge from the $C \leftrightarrow (\Delta E)^2$ relation by a factor proportional to $1/T$. Equation (6) explains why many MD simulations give good agreement with the equipartition theorem for average energies in thermal equilibrium, while Eq. (9) explains why fluctuations have an excess term, as shown in FIG. 2 (B). Equation (9) also explains why excess fluctuations onset abruptly when nnn atoms begin to interact, $b \neq 0$, as found for MD simulations at low T [6].

Quantitative comparison with the MD simulations in FIG. 2 can be made by evaluating the L-J model. The L-J potential energy as a function of radial distance (r) is $u(r) = 4\epsilon_{LJ}[(\sigma/r)^{12} - (\sigma/r)^6]$. For argon atoms, the energy scale is $\epsilon_{LJ}/k_B = 118.2$ K and the length scale is $\sigma = 0.3405$ nm [30]. The potential energy has its minimum ($u_{nn} = -\epsilon_{LJ}$) at the nn distance of $r_{nn} = 2^{1/6}\sigma$, and a value of $u_{nnn} = -15\epsilon_{LJ}/64$ at the nnn distance of $r_{nnn} = 2^{2/3}\sigma$. Expanding the potential energy to quadratic order about r_{nn} , the interaction between nn atoms is $u(r_{nn} + \delta r) = \epsilon_{LJ}[-1 + 36(\delta r)^2/(2^{1/3}\sigma^2)]$. From the geometry in FIG. 3 (A), δr is $\pm x/\sqrt{2}$, where x is the displacement of the central atom from the origin along the X -axis. The 4 atoms in the Y - Z plane do not contribute, leaving 8 of the 12 nn atoms that add equally to the quadratic term. The net potential energy is

$$u_{fcc}(r_{nn} + x) = \epsilon_{LJ} \left(-12 + \frac{144}{2^{1/3}\sigma^2} x^2 \right). \quad (10)$$

Thus, the factor for the harmonic term in the L-J potential is $a = 144\epsilon_{LJ}/(2^{1/3}\sigma^2)$. For each nnn atom at distance r_{nnn} , to linear order, the potential is $u(r_{nnn} + \delta r) = \epsilon_{LJ}[-15/64 + 21\delta r/(2^{14/3}\sigma)]$. In the fcc lattice there are 6 nnn atoms that can be grouped into opposing pairs displaced by δx_{\pm} , as shown in FIG. 3 (A). The net potential energy becomes

$$u_{fcc}(r_{nnn} + \delta x_+ - \delta x_-) = \epsilon_{LJ} \left[-\frac{45}{32} + \frac{63}{2^{14/3}\sigma} (\delta x_+ - \delta x_-) \right]. \quad (11)$$

Thus, the main factor modulating the energies of the L-J model is $b = -63\epsilon_{LJ}/(2^{14/3}\sigma)$. We neglect all higher-order terms.

Due to its quadratic dependence on momentum, fluctuations in kinetic energy in the x -direction are $(\bar{\Delta}k)^2 = (\Delta k)^2 = (k_B T)^2/2$. From Eq. (9), the excess fluctuations for the L-J model are:

$$\frac{(\bar{\Delta}u)^2}{(\bar{\Delta}k)^2} - 1 = \frac{b^2}{ak_B T} = \frac{21^2}{2^{13}} \frac{\epsilon_{LJ}}{k_B T} \approx 0.053833 \frac{\epsilon_{LJ}}{k_B T}. \quad (12)$$

Because each degree of freedom adds equally to both k and u , Eq. (12) also holds in 3-dimensions. The prefactor in Eq. (12) is in excellent agreement with $\eta = 0.054 \pm 0.004$ from the simulations in FIG. 2. This agreement implies that contributions from neighbors farther than nnn can be neglected.

Equation (12) is for individual atoms. Most results from the MD simulations involve net fluctuations of cube-shaped blocks containing $n \gg 1$ atoms. Denote the total kinetic and potential energies of each block by K and U , respectively. Fluctuations of kinetic energy are extensive, $(\bar{\Delta}K)^2 \propto n$. Adapting Eq. (1), a theoretical expression for the n -dependence of excess fluctuations is

$$\frac{(\bar{\Delta}U)^2}{(\bar{\Delta}K)^2} - 1 = \eta n^{\gamma-1} \frac{\epsilon_{LJ}}{k_B T}. \quad (13)$$

From Eq. (1), $\gamma \approx 0.75$. The nonextensive size dependence on the right-hand side is significant over a wide range of block sizes. For the L-J model at $T = 0.1$ K, nonextensive fluctuations dominate over extensive ones if $n < 10^7$.

We propose that Eq. (13) can be interpreted by analogy with diffusion. If n is regarded as the number of time steps in random walk, in the limit of very large systems there is normal diffusion, while the nonextensive behavior shown in FIG. 2 (B) corresponds to subdiffusion [31]. Here, we describe the nonextensive relation in terms of random walk on random walk [32,33]. For modulations of the energy of the i -th atom that yield the excess fluctuations, we consider the variable $U_i^c = W_i \sin \Phi_i$, where both W_i and Φ_i are random, with W_i made

dimensionless for simplicity. We identify $(\Delta U^c)^2$ with the excess-fluctuation part, leaving the specific distributions of W and Φ to be found. This form of U^c is guided by Eq. (5). First, let us define $\Psi \equiv \sum_{i=1}^n \Psi_i$ ($\Psi_i = \sin \Phi_i$) and $W \equiv \sum_{i=1}^n W_i$. The joint probability of finding ψ and w as the realizations of Ψ and W at the n -th step is $P_n(\psi, w) = p_n(w|\psi)p_n(\psi)$. If Ψ_i 's are independent and identically distributed, then Ψ may be assumed to obey the binomial distribution that can be approximated by the Gaussian distribution

$$p_n(\psi) = \frac{1}{2^n} \frac{n!}{\left[\frac{1}{2}(n+\psi)\right]! \left[\frac{1}{2}(n-\psi)\right]!} \approx \frac{1}{\sqrt{2\pi n}} \exp\left(-\frac{\psi^2}{2n}\right). \quad (14)$$

The joint distribution and Eq. (14) are integrated over a range of values to obtain the net mean-squared deviations of U^c . Assuming large enough block sizes (but still $n < 10^7$), the range of integration can be extended to $(-\infty, \infty)$. Since the distributions are even functions, the average of U^c vanishes. Then, if the conditional probability distribution is taken to be

$$p(w|\psi) = \frac{|\psi|^{1/4}}{\sqrt{2\pi}} \exp\left(-\frac{\sqrt{|\psi|}w^2}{2}\right), \quad (15)$$

which is independent of n , mean-squared fluctuations become

$$\begin{aligned} (\Delta U^c)^2 &= \int_{-\infty}^{\infty} d\psi \int_{-\infty}^{\infty} dw \psi^2 w^2 p_n(\psi) p_n(w|\psi) \\ &= \frac{\Gamma(5/4)}{\sqrt{\pi}} (2n)^{3/4}, \end{aligned} \quad (16)$$

Although the dashed lines in FIG. 2 show good agreement with the size dependence of Eq. (16), the validity of the joint distribution in Eq. (15) should be examined by future work.

We now seek to extend our theory of excess fluctuations in simulations to excess specific heat in measurements. Note their qualitative similarity: FIG. 1 shows that measured specific heats diverge from Debye's theory as $1/T \rightarrow 0$ via $C/T^3 \propto 1/T^\mu$ with $\mu = 0.94 \sim 1.64$, while FIG. 2 shows a similar divergence for excess fluctuations $(\bar{\Delta}U)^2/(\bar{\Delta}K)^2 - 1 \propto 1/T^\mu$ with $\mu = 1$. The simulations are purely classical, whereas low-temperature measurements involve quantum effects. We use the basic idea that semiclassical anharmonic terms from nnn atoms modulate the energies of the quantized harmonic modes from Debye's theory.

Let ε be the energy of a phonon, with ε_m the maximum (cut-off) energy in Debye's theory. A textbook expression [7] for the temperature-dependent part of the thermal average energy of N atoms at low T is

$$E = \frac{9N}{\varepsilon_m^3} \int_0^\infty d\varepsilon \varepsilon^2 \left(\frac{\varepsilon}{e^{\varepsilon/k_B T} - 1} \right). \quad (17)$$

We modify Eq. (17) by introducing energy modulations

$$c_\lambda(t) = \mathcal{A}_\lambda [\sin(\omega t + \alpha) - \sin \omega t], \quad (18)$$

$$\mathcal{A}_\lambda = \kappa_\lambda (k_B T)^{\lambda/2}, \quad (19)$$

where κ_λ is a T -independent positive constant. In the classical limit, $\lambda = 1$ and $\kappa_1 = 1/\sqrt{2a}$, Eq. (19) yields Eq. (4) for oscillations that depend linearly on T via the equipartition theorem. In the low- T quantum limit, $\lambda = 0$ in Eq. (19) is identified with zero-point oscillations so that \mathcal{A}_0 is independent of T . Intermediate values, in the range $0 < \lambda < 1$, may be identified with semiclassical behavior. Although further work will be needed to fully quantize the modulations, here we examine how the semiclassical approach may qualitatively describe the measured deviations from Debye's theory.

The density of states can be changed to include the modulation, analogous to a standard treatment (e.g. chapter 14 in Ref. [34]). As in our theory for classical MD simulations, explained earlier, we assume that the modulations are localized around each atom and decoupled from the heat bath. Such localized modes are consistent with measurements of localized normal modes [23-28] and reduced correlations between nnn atoms in crystals [29].

Following the procedure used for Eq. (8), the time- and phase-averages (again denoted by an overbar) are taken before the thermal average to obtain the equilibrium quantity. Then, using $\widehat{H}_\lambda = \varepsilon \hat{n} + c_\lambda(t)$ (where the number operator, \hat{n} , has eigenvalues $n = 0, 1, 2, \dots$) as the modulated single-atom Hamiltonian, Eq. (17) must be modified as

$$E_\lambda = \int_0^\infty d\varepsilon \overline{D(\varepsilon + c_\lambda(t))} \times \overline{\langle \widehat{H}_\lambda \rangle_{th}}, \quad (20)$$

where $D(\varepsilon) = (9N/\varepsilon_m^3)\varepsilon^2$ is the density of states. Using the density matrix $\hat{\rho} = \exp(-\varepsilon \hat{n}/k_B T) / Z$ with $Z = Tr \exp(-\varepsilon \hat{n}/k_B T) = 1/[\exp(\varepsilon/k_B T) - 1]$, the thermal average of $\widehat{H}_\lambda = \varepsilon \hat{n}$ is $\overline{\langle \widehat{H}_\lambda \rangle_{th}} = Tr(\overline{\widehat{H}_\lambda} \hat{\rho}) = \varepsilon / (e^{\varepsilon/k_B T} - 1)$. The internal energy becomes

$$\begin{aligned} E_\lambda &= \frac{9N}{\varepsilon_m^3} \int_0^\infty d\varepsilon (\varepsilon^2 + b^2 \mathcal{A}_\lambda^2) \frac{\varepsilon}{e^{\varepsilon/k_B T} - 1} \\ &= \frac{9N}{\varepsilon_m^3} \left[6 \frac{\pi^4}{90} (k_B T)^4 + \frac{\pi^2}{6} (k_B T)^2 b^2 \mathcal{A}_\lambda^2 \right]. \end{aligned} \quad (21)$$

The dimensionless specific heat per atom becomes

$$\frac{C}{k_B} \approx \frac{9}{\varepsilon_m^3} \left[\frac{4\pi^4}{15} (k_B T)^3 + \frac{\pi^2}{6} (\lambda + 2) b^2 \kappa_\lambda^2 (k_B T)^{\lambda+1} \right]. \quad (22)$$

This result predicts an excess specific heat added to Debye's T^3 -law, which varies as $C \propto T^{\lambda+1}$, consistent with measured excess specific heats having $0 \lesssim \lambda \lesssim 1$. Comparing this to the exponent, μ , in FIG. 1, we have the relation: $\lambda + \mu = 2$. Using the classical values, $\lambda = 1$ and $\kappa_1 = 1/\sqrt{2a}$, with parameters for the argon lattice in the L-J model, $a =$

$(144/2^{1/3}) \epsilon_{LJ}/\sigma^2$ and $b = -(63/2^{14/3}) \epsilon_{LJ}/\sigma$, Eq. (22) predicts a crossover from Debye's T^3 behavior to excess $C \propto T^2$ at

$$\begin{aligned} T &= \frac{1}{k_B} \left[\frac{5}{8\pi^2} (\lambda + 2) b^2 \kappa_1^2 \right]^{1/(2-\lambda)} \\ &= \frac{15}{16\pi^2} \left(\frac{63}{2^{14/3}} \right)^2 \frac{2^{1/3}}{144} \frac{\epsilon_{LJ}}{k_B}, \end{aligned} \quad (23)$$

which is about 0.60 K. Measured specific heats of argon [35] down to $T \approx 0.40$ K do not exhibit any clear deviations from the T^3 -law. However, this is not surprising because the purely classical treatment is not expected to be valid at such low temperatures. Indeed, FIG. 1 shows that the measured temperature exponent of the excess specific heat is $1 \lesssim \mu \lesssim 2$, consistent with $0 \leq \lambda \leq 1$. Another factor altering the crossover is that most phonons at such low T are primarily in-phase, decreasing the amplitude of the out-of-phase mode from our proposal of random atomic motions. Using interaction parameters for other crystals, such as those in FIG. 1, will clarify the connections between experiment and theory.

In summary, at very low temperatures, the excess specific heat measured in high-purity single crystals (FIG. 1) is similar to the excess energy fluctuations found in MD simulations of ideal crystals (FIG. 2), suggesting a common mechanism. The simulations are quantitatively characterized (dashed lines in FIG. 2) by a theory for anharmonic interactions between next-nearest-neighbor (nnn) atoms (FIG. 3). This theory involves independent fluctuations of nnn atoms that modulate the energies of harmonic motions. We present a novel method for treating the modulations by combining time- and phase-averaging with thermal averaging, but with careful attention to the order of averaging. Equation (9) gives a correction term to the canonical-ensemble connection between fluctuations and specific heat, the $C \leftrightarrow (\Delta E)^2$ relation. We extend our theory of energy modulations to Debye's theory of phonons. The results, given in Eqs. (21) and (22), provide a qualitative explanation for the excess specific heat and excess energy fluctuations measured in crystals and glasses.

Acknowledgments: RVC has benefited from discussions with T. J. Newman. SA is supported by a grant from National Natural Science Foundation of China (No. 12375031).

REFERENCES

- [1] D. G. Cahill and R. O. Pohl, Lattice vibrations and heat transport in crystals and glasses, *Ann. Rev. Phys. Chem.* **39**, 93 (1988).
- [2] D. W. Rogers, *Einstein's Other Theory: The Planck-Bose-Einstein Theory of Heat Capacity* (Princeton University Press, Princeton, 2005).
- [3] W. Knaak and M. Meissner, Time-resolved specific heat measurements on high-purity single crystals between 50 mK and 1 K, in *Proceedings of the 17-th International Conference on Low Temperature Physics*, edited by U. Eckern, A. Schmid, W. Weber, and H. Wühl (North Holland, Amsterdam, 1984), p. 667.
- [4] J. J. De Yoreo, W. Knaak, M. Meissner, and R. O. Pohl, Low-temperature properties of crystalline $(\text{KBr})_x(\text{KCN})_x$: A model glass, *Phys. Rev. B* **34**, 8828 (1986).
- [5] N. Sampat and M. Meissner, Time-dependent specific heat of crystals and glasses at low temperatures, pgs. 105-112 in *Die Kunst of Phonons*, eds. Paszkiewicz, T., Rapcewicz, K., Plenum Press (1994).
- [6] R. V. Chamberlin, V. Mujica, S. Izvekov, and J. P. Larentzos, Energy localization and excess fluctuations from long-range interactions in equilibrium molecular dynamics, *Physica A* **540**, 123228 (2020).
- [7] T. L. Hill, *An Introduction to Statistical Thermodynamics* (Addison Wesley, Reading MA, 1960).
- [8] M. T. Loonen, R. C. Dynes, V. Narayanamurti, and J. P. Garno, Measurements of time-dependent specific heat of amorphous materials, *Phys. Rev. B* **25**, 1161 (1982).
- [9] B. Schiener, R. Böhmer, A. Loidl, and R. V. Chamberlin, Nonresonant spectral hole burning in the slow dielectric response of supercooled liquids, *Science* **274**, 752 (1996).
- [10] R. V. Chamberlin, Nonresonant spectral hole burning in a spin glass, *Phys. Rev. Lett.* **83**, 5134 (1999).
- [11] R. C. Zeller and R. O. Pohl, Thermal conductivity and specific heat of noncrystalline solids, *Phys. Rev. B* **4**, 2029 (1971).
- [12] P. W. Anderson, B. I. Halperin, and C. M. Varma, Anomalous low-temperature thermal properties of glasses and spin glasses, *Phil. Mag.* **25**, 1 (1972).
- [13] W. A. Phillips, Tunneling states in amorphous solids, *J. Low Temp. Phys.* **7**, 351 (1972).
- [14] M. A. Ramos, Are universal “anomalous” properties of glasses at low temperatures truly universal? *Low Temp. Phys.* **46**, 104 (2020).
- [15] C. C. Yu and H. M. Carruzzo, Two-level systems and the tunneling model: A critical review, in *Low-temperature thermal and vibrational properties of disordered solids* ed. by M. A. Ramos, (World Scientific, London, 2022). p. 113.
- [16] D. Szewczyk et al., Specific heat at low temperatures in quasiplanar molecular crystals: Origin of glassy anomalies in minimally disordered crystals, *Phys. Rev. B* **110**, 174204 (2024).
- [17] Burnett, J. et al., Evidence for interacting two-level systems from the $1/f$ noise of a superconducting resonator, *Nat. Commun.* **5**, 4119 (2014).
- [18] S. Kempf, A. Ferring, and C. Enss, Towards noise engineering: Recent insights into low-frequency excess flux noise of superconducting quantum devices, *Appl. Phys. Lett.* **109**, 162601 (2016).
- [19] S. Pirro and P. D. Mauskopf, Advances in bolometer technology for fundamental physics, *Annu. Rev. Nucl. Part. Sci.* **67**, 161 (2017).
- [20] N. P. de Leon et al., Materials challenges and opportunities for quantum computing hardware, *Science* **372**, 2823 (2021).

-
- [21] A. M. J. Zwerver et al., Qubits made by advanced semiconductor manufacturing, *Nat. Elect.* **5**, 184 (2022).
- [22] A. J. Leggett and D. C. Vural, “Tunneling two-level systems” model of the low-temperature properties of glasses: Are “smoking-gun” tests possible?, *J. Phys. Chem. B* **117**, 12966 (2013).
- [23] R. Jankowiak and G. J. Small, Hole-burning spectroscopy and relaxation dynamics of amorphous solids at low temperatures, *Science* **237**, 618 (1987).
- [24] U. Buchenau, Y. M. Galperin, and V. L. Gurevich, Anharmonic potentials and vibrational localization in glasses, *Phys. Rev. B* **43**, 5039 (1991).
- [25] D. Engberg et al., Sound waves and other modes in the strong glass former B₂O₃, *Phys. Rev. B* **58**, 9087 (1998).
- [26] W. E. Moerner, Examining nanoenvironments in solids on the scale of a single, isolated impurity molecule, *Science* **265**, 46 (1994).
- [27] E. Vidal Russell and N. Israeloff, Direct observation of molecular cooperativity near the glass transition, *Nature* **408**, 695 (2000).
- [28] E. Flenner and G. Szamel, The origin of sound damping in amorphous solids: Defects and beyond, *Sci. Adv.* **11**, 6097 (2025).
- [29] I. K. Jeong, R. H. Heffner, M. J. Graf, and S. J. L. Billinge, Lattice dynamics and correlated atomic motion from the atomic pair distribution function, *Phys. Rev. B* **67**, 104301 (2003).
- [30] J. A. White, Lennard-Jones as a model for argon and test of extended normalization group calculations, *J. Chem. Phys.* **111**, 9352 (1999).
- [31] J. P. Bouchaud and A. Georges, Anomalous diffusion in disordered media: statistical mechanisms, models and physical applications, *Physica* **195**, 127 (1990).
- [32] K. W. Kehr and R. Kutner, Random walk on a random walk, *Physica* **110A**, 535 (1982).
- [33] L. Turban, Iterated random walk, *Europhys. Lett.* **65**, 627 (2004).
- [34] C. Kittel, *Introduction to Solid State Physics*, 5th edition, Chapter 14, (Wiley, New York, NY, 1976).
- [35] L. Finegold and N. E. Phillips, Low-temperature heat capacities of solid argon and krypton, *Phys. Rev.* **177**, 1383 (1969).